2013

Direct observation of liquid-like behavior of a single Au grain boundary

Gilberto Casillas
University of Texas at San Antonio, gilberto@uow.edu.au

Arturo Ponce
University Of Texas At San Antonio

Jesus Velazquez-Salazar
University Of Texas At San Antonio

M Jose-Yacaman
University of Texas at San Antonio

Publication Details

Casillas, G., Ponce, A., Velazquez-Salazar, J. J. & Jose-Yacaman, M. (2013). Direct observation of liquid-like behavior of a single Au grain boundary. Nanoscale, 5 (14), 6333-6337.

Direct observation of liquid-like behavior of a single Au grain boundary

Abstract
Behavior of matter at the nanoscale differs fromthat of the bulk due to confinement and surface effects. Here, we report a direct observation of liquid-like behavior of a single grain boundary formed by cold-welding Au nanoparticles, 40 nm in size, by mechanical manipulation in situ TEM. The grain boundary rotates almost freely due to the free surfaces and can rotate about 90 degrees. The grain boundary sustains more stress than the bulk, confirming a strong bonding between the nanoparticles.Moreover, this technique allows the measurement of the surface diffusion coefficient from experimental observations, which we compute for the Au nanoparticles. This methodology can be used for any metal, oxide, semiconductor or combination of them.

Keywords
grain, direct, observation, au, liquid, single, like, behaviour, boundary

Disciplines
Engineering | Physical Sciences and Mathematics

Publication Details
Casillas, G., Ponce, A., Velazquez-Salazar, J. J. & Jose-Yacaman, M. (2013). Direct observation of liquid-like behavior of a single Au grain boundary. Nanoscale, 5 (14), 6333-6337.

Nanoscale

RSC Publishing

COMMUNICATION

Direct observation of liquid-like behavior of a single Au grain boundary†

Cite this: *Nanoscale*, 2013, **5**, 6333

Gilberto Casillas, Arturo Ponce, J. Jesús Velázquez-Salazar and Miguel José-Yacamán*

Received 26th March 2013
Accepted 29th May 2013

DOI: 10.1039/c3nr01501g

www.rsc.org/nanoscale

Behavior of matter at the nanoscale differs from that of the bulk due to confinement and surface effects. Here, we report a direct observation of liquid-like behavior of a single grain boundary formed by cold-welding Au nanoparticles, 40 nm in size, by mechanical manipulation *in situ* TEM. The grain boundary rotates almost freely due to the free surfaces and can rotate about 90 degrees. The grain boundary sustains more stress than the bulk, confirming a strong bonding between the nanoparticles. Moreover, this technique allows the measurement of the surface diffusion coefficient from experimental observations, which we compute for the Au nanoparticles. This methodology can be used for any metal, oxide, semiconductor or combination of them.

It is well known that free surfaces play a key role in defining properties of matter at the nanoscale. As matter goes down in size, the role of free surfaces becomes increasingly relevant, changing their properties compared to their bulk counterparts. Regarding mechanical properties, Zheng *et al.*[1] showed that free surfaces impact the mechanical properties of nanomaterials as they act as sources and sinks of dislocations. Moreover, grain boundaries (GBs) also affect the overall properties of the materials; *e.g.*, twin boundaries present a small resistance for electron conduction, while at the same time it enhances the mechanical properties of the material.[2] Most of the studies of GBs have been done in thin films where the free surfaces are hard to account for and most of the times the models used to analyze them disregard free surfaces due to a small surface/volume ratio.

There are also studies of triple junction between free surfaces and GBs that include surface effects.[3,4] However, two-dimensional models are used as a simplification of the problem. Conventional studies of GB or interfaces can only infer the processes involved in the experiments; in addition, since the interface is buried, direct observation of friction experiments are rare. Some works have studied the effect of free surfaces in the migration and rotation of GBs in thin films barely mentioning the role of the free surfaces.[5,6] Particularly, Derlet and Swygenhoven[7] studied the effect of free surfaces and demonstrated that they change the plastic deformation of materials.

In situ TEM studies have enabled the ability to observe dynamical process during mechanical deformation in polycrystalline thin films.[8–11] Single metal–metal contacts were studied recently in Ag[12] and Au[13] by a cold-welding process, which consisted in the application of a bias voltage to induce the welding. Moreover, a cold-welding technique without an applied bias was also reported by Lu *et al.*[14] where they were able to weld ultrathin Au nanowires thanks to a similar crystallographic orientation between nanowires. A more detailed study of Au–Au contacts was done by Merkle and Marks,[15] where they observed a liquid-like behavior between the gold contacts, resulting in necking after pulling or shearing of the contacts, however, the contact interface was not clearly observed. More recently, Wakai *et al.*[16] used focused-ion-beam-machined samples to study the sintering of single GBs of two Au grains by annealing in the micron-size regime. However, most of these studies lacked spatial resolution to clearly observe what was happening at the contact point.

Herewith, we report an experimental observation of the liquid-like behavior of a single GB at the nanoscale. By taking advantage of the piezo-controlled stage in the *in situ* holder (AFM-TEM holder from Nanofactory Inc.), we were able to manipulate the GB between two nanoparticles (NPs) by controllably displacing one of the nanoparticles while directly observing the contact region. The GB was able to freely rotate (up to 90 degrees). Moreover, this new methodology can be used to study individual GBs of any kind of NPs (under 50 nm) and compute the surface diffusion coefficient of the material by *in situ* TEM observation. We demonstrate this by measuring the surface diffusion coefficient in the studied 40 nm Au NPs. Briefly, the experiment consisted in picking up a NP by applying

Department of Physics and Astronomy, University of Texas at San Antonio, One UTSA Circle, San Antonio, Texas 78249, USA. E-mail: miguel.yacaman@utsa.edu

† Electronic supplementary information (ESI) available. See DOI: 10.1039/c3nr01501g

a load with the Si tip until the NP was attached to the tip. After the particle is attached to the Si tip, another particle is approached to the tip-attached Au NP and they are brought to contact, while recording the experiment in a CCD camera. For clarification, the particle attached to the Si tip is marked as "Fixed" in each figure, while the other particle is manually moved by the piezo. See ESI† for more details.

Fig. 1 shows a sequence of two NPs coming into contact (shown in full in ESI video 1†). After the particles weld together and form a GB, a neck region was formed around 17 nm in diameter. No stress was applied to force the welding; the bottom-left particle was moved in the in-plane direction until it came into contact with the other particle and left unmoved for a few seconds. After the particles touched (Fig. 1b) a neck region formed and grew from 17 nm to 24 nm by surface diffusion after 17 seconds. This changed the dihedral angle at the junction of the GB and the free surfaces, bringing to equilibrium the surface energy and GB energy. After reaching an equilibrium contact between the two particles, the bottom particle was moved perpendicularly with respect to the "Fixed" particle. During the tangential movements, the GB changed instantly in a liquid-like behavior. This is more clearly observed in the real time video (see ESI video 1†) since the small fluctuations are too fast to appreciate in the individual frames. Merkle and Marks[15] showed a liquid-like behavior of gold contacts at a temperature of 166 °C by applying a bias, however, our experiments were performed at room temperature and no bias was applied, showing that the liquid like behavior that Pashley *et al.*[17] observed also happens at room temperatures. Fig. 2 shows four states of the same GB in Fig. 1 as it changed with movement and time (see ESI video 1†). In Fig. 2a the bottom particle was moved to the left causing the GB to rotate +11 (clockwise rotation is considered positive, while counterclockwise is considered negative) with respect to the initial angle in Fig. 1d (marked by a solid line) enlarging the diameter of the GB to 27 nm.

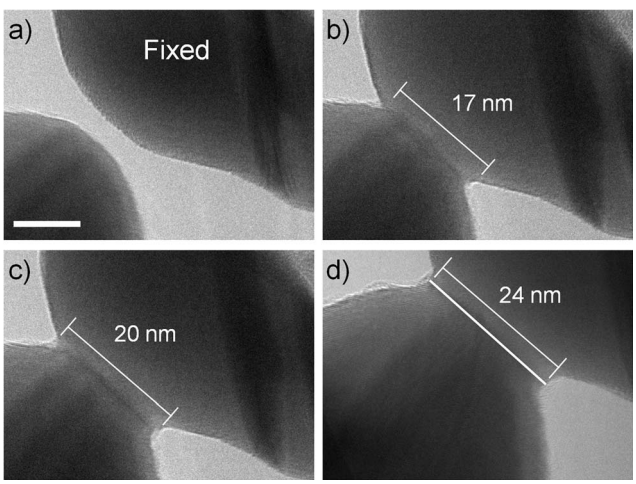

Fig. 1 Sequence of TEM images of the broadening of the contact region between two NPs. (a) Particles before contact at 0 s. (b) Neck region at 17 nm in size at 1.33 s. (c) Neck region 20 nm in size at 2.73. (d) Neck region 24 nm in size at 12.47 s. Solid line in (d) is used as a reference for Fig. 2. Scale bar is 10 nm. (See ESI video 1†).

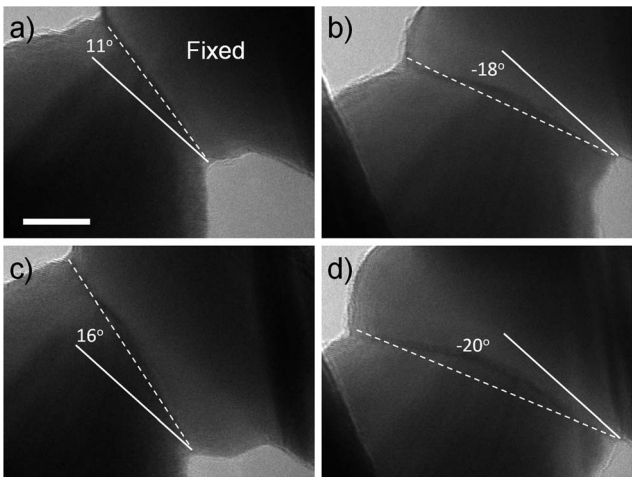

Fig. 2 Sequence of TEM images of the migration and rotation of the GB. The solid line is used as a reference comparing to Fig. 1d. The GB is rotated 11° (a) (16.33 s), −18° (b) (19.73 s), 16° (c) (27.4 s) and −20° (d) (36.73 s) back and forth without breaking. Scale bar is 10 nm. (See ESI video 1†).

Afterwards, the bottom particle was moved in the opposite direction and the GB rotated again −18 degrees (with respect to Fig. 1d) without breaking. The size of the GB increased to 34 nm, while the shape of the NPs changed due to reorganization of the surfaces by the movement of the GB. As the GB moves and leaves behind a free surface, this surface becomes more rounded to minimize surface energy. This movement could be repeated, as shown in Fig. 2c and d where the GB rotates +16 and −20 degrees from the initial position (Fig. 1d) and increases up to 42 nm in diameter approx. Moreover, the shape of the grains (NPs) changed significantly by the increased rotation of the GB; more interestingly, the size of the NPs also changed. Atoms near the GB change in crystal orientation from one grain to the other, changing the actual size (and shape) of each NP due to the repeated motion of the NP causing the migration of the GB towards the bottom NP.

Fig. 3 shows a sequence of lower magnification images of the same two particles in Fig. 1 and 2 (ESI videos 1†). First, notice that in Fig. 3a the GB is almost at the starting angle in Fig. 1d, then, from Fig. 3a to b the bottom NP was moved in the top-left direction causing the GB to slide revealing free surfaces where the GB used to be (marked by an arrow). The top part of the GB almost reached the silicon tip, limiting the diffusion of the GB, making it more favorable for the GB to slide in its own plane than to keep rotating. Moreover, by moving the NP in the opposite direction (bottom right) the GB slid back into the original position and then rotated again counterclockwise (Fig. 3c). The movement of the GB is not restricted to an edge-on orientation. Fig. 3d shows the GB after moving the bottom nanoparticle in the direction of the electron beam, changing the plane of the GB of an almost edge-on view to a tilted view (arrows mark contrast fringes of the GB). Finally, the bottom particle was moved from right to left (Fig. 3e) until the top particle detached from the Si tip (Fig. 3f). As mentioned before, the size of the grains changed from Fig. 3a to e. Cahn and Taylor[18] proposed that coupling of grain rotation and relative

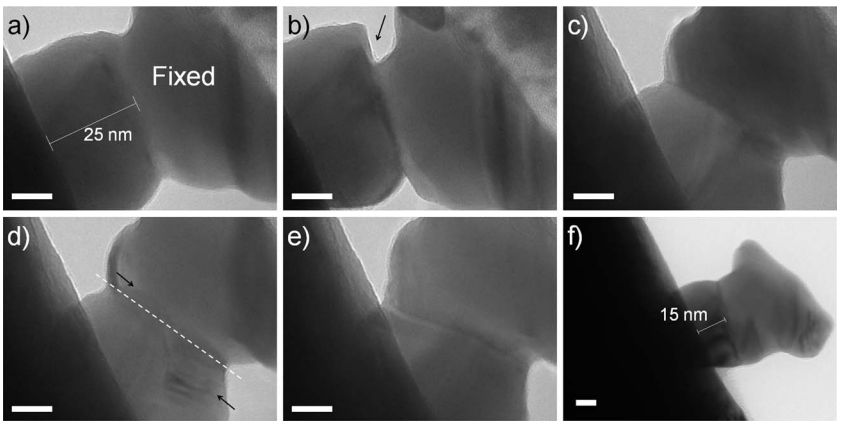

Fig. 3 Sequence of TEM images of the GB rotating and sliding. (a) GB at 69.27 s. (b) The NPs slid, leaving a surface of the bottom-left particle (marked by an arrow) (70.87 s). (c) The GB is moved back covering the free surface left open in (b) and rotates counterclockwise (76.666 s). (d) The bottom particle is moved towards the beam direction and contrast fringes can be observed as the GB moves (marked by arrows) (80.8 s). (e) The GB is moved back to an almost on-edge view (84.47 s). (f) The NPs detached from the Si tip. (120 s). Scale bars are 10 nm. (See ESI video 1†).

tangential movement would occur if an external stress was applied to the material; however, in this experiment both NPs are fixed, and therefore cannot rotate. Instead, one NP is moved (bottom) relative to the other one ("Fixed"), which is analogous to rotate the grain; and instead of changing the orientation of the GB in the same plane, the GB rotated to compensate the motion of the NPs. Moreover, after all the rotations of the GB, there was a net motion in the direction of the tip, towards the bottom NP, which shrank 10 nm along the tip direction.

While the applied stress is the driving force for the migration of the GB, displacement of atomic planes can also occur if the stress is applied in the appropriate direction; on the other hand, if the direction is not favorable, the crystal planes will distort and can create a new grain. Fig. 4a shows a different set two NPs that just came into contact (see ESI video 2†). Moving the bottom NP (similar to Fig. 1–3) the GB rotates clockwise, causing a stress upwards on the left part of the top NP displacing several atomic planes in the process (marked with an arrow in Fig. 4b). In this case the (111) planes are in a direction parallel to the stress, facilitating the shear of the planes with the GB movement, which would mean an increased stress if the slip planes are perpendicular to the GB movement. In Fig. 4c the bottom particle was moved in the bottom-right direction rotating the GB to an almost horizontal position (12 degrees from the horizontal direction). Also, the GB reached a maximum rotation and started slipped due to the reduced size of the bottom NP. From Fig. 4d to l the bottom NP was moved to the left, causing the GB to rotate 85 degrees (7 degrees clockwise from the vertical direction). To our knowledge, such a behavior has not been reported before. Moreover, From Fig. 4e to i, a step-wise migration of the GB is observed. In Fig. 4e three steps in the GB are clearly visible; which then move to the left part of the GB as the bottom NP is moved to the left (Fig. 4f marked with numbers). In Fig. 4g the first step already disappeared in the surface while the second and third steps are still visible, which finally disappear in Fig. 4i.

Furthermore, in Fig. 4i it is possible to observe, by the change in the phase contrast (marked by an arrow), a region of accumulated strain. This is evidenced by the 10 degrees rotation of the lattice planes at both sides of the strained region. In Fig. 4j a dislocation is already visible, resulting in a rotation of 15 degrees between planes at both sides of the dislocation. In Fig. 4k the angle is about 22 making it a new grain which disappeared rather fast (2 seconds later), due to the small size and the stress driven by the two GBs. Finally, in Fig. 4l the GB ended up rotated 85 degrees compared to Fig. 4c, demonstrating the diffusivity in the presence of free surfaces of GBs in Au. To test the strength of the GB, a stress of 180 MPa (yield stress for bulk Au is about 25 MPa (ref. 19)) was applied to the NPs after the bottom one detached from the Au support; however, the NPs were left intact with no signs of plastic deformation after loading (see ESI video 3†).

It is important to notice that it is not necessary to heat the NPs in order to weld them; the experiments were performed at room temperature, similar to the work of Lu *et al.*[14] As they also discuss in their work, heating due to the electron beam can be disregarded for several reasons. The experiments were performed under low-intensity-spread electron beam illumination (less than 10 pA cm^{-2}); therefore, the change in temperature is small enough to be disregarded. According to Rez and Glaisher,[20] the increment in temperature decreases as the NP size increases. In a different work, José-Yacamán *et al.*[21] reported a maximum increase of 10 K in 2 nm NPs, confirming that in our case, due to the size of the NPs, the temperature increase is small enough to disregard its effects. Furthermore, heating due to electron beam is only relevant when there is poor thermal contact between the NPs and the substrate; in our case, the substrate is gold, ensuring good electrical and thermal conductivity. Fig. S2† shows the NPs in Fig. 4 before contact for a period of 40 s, where the morphology of the NP on the right does not change under the electron beam, further confirming that the electron beam does not have significant effect on NPs.

Lu *et al.*[14] concluded that a combination of surface diffusion and formation of adatoms in the surfaces, plus crystal orientation, allowed for such cold-welding process. In our experiment, the NPs are randomly oriented and still the cold welding

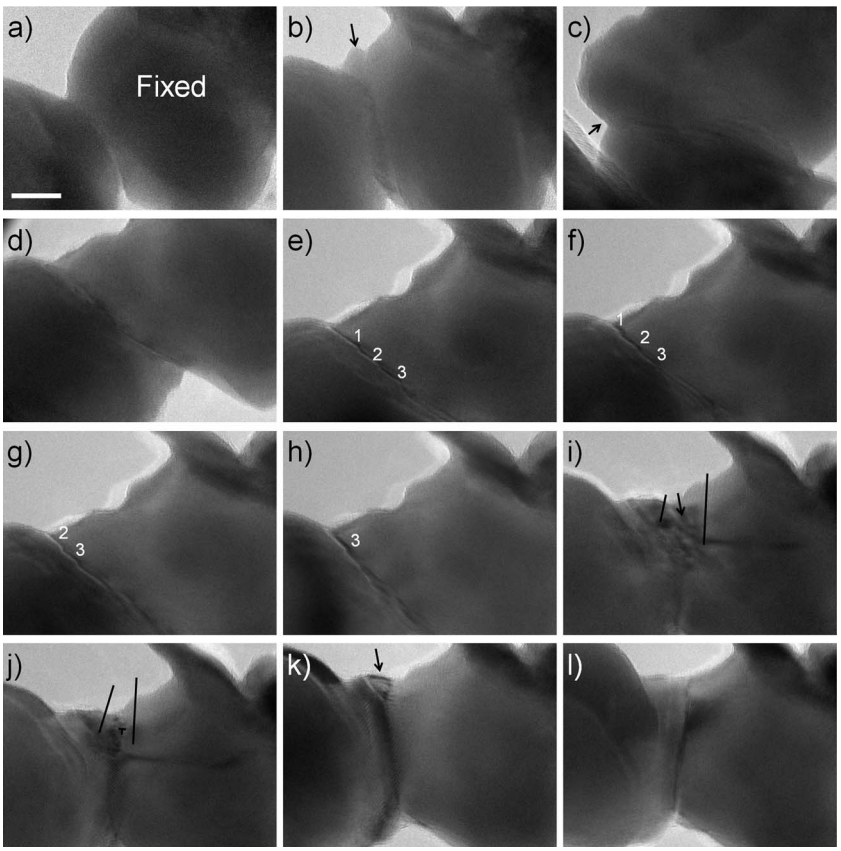

Fig. 4 Sequence of TEM images of a moving GB. (a) The particles come into contact (0 s). (b) The bottom left particle is moved to the top left direction rotating the GB and causing the slip of a few atomic planes (marked by the arrow) (18.47 s). (c) The bottom left particle is moved to the right direction all the way until the GB glides leaving free surfaces (marked by the arrow) (46.33 s). (d) The bottom particle is moved to the left (49.67 s). (e–h) The bottom left particle is moved in the top left direction where a rotation of the GB in steps can be observed (marked by numbers) ((e) is 54 s, (f) is 55.2 s, (g) is 60 s and (h) is 61.47 s). (i) A stressed region is observed (marked by an arrow) and is evidenced by the 10° rotation of the Au planes (67.07 s). (j) The stress builds up and the planes rotate 15° (67.8 s). (k) A third grain is formed by the movement of the left particle (marked by an arrow) (70.73 s). (l) The small grain disappears and the GB is rotated even further (83.933 s). Scale bar is 10 nm. (See ESI video 2†).

process was easy and fast. Actually, there is an attraction force between the NPs before they touched each other, meaning that we did not have to apply any stress to the NPs in order to weld. The mechanical manipulation initializes the cold welding process followed by a rapid diffusion of surface atoms due to the junction between the free surfaces and the GB, regarding relative orientation between the NPs. After the surface tension and GB energy reached equilibrium, the GB was stable enough to withstand the relative movements of the NPs by reorganizing the atoms in the boundary. Fig. S1† shows dark field (DF) images of the final state of the NPs in Fig. 3f. In Fig. S1b and c† two different diffracted spots are selected to confirm the different crystallographic orientation of the two grains, while in Fig. S1d† a diffracted spot corresponding only to the GB is chosen, revealing that the GB crystal structure does not correspond to either of the two grains. This behavior remarks the role of the free surfaces in the evolution of GBs, while this is the simplest case to be studied where only one GB interacts with free surfaces. The effect of the relative crystallographic orientations of the NPs is beyond this paper, but it is expected to be relevant since the GBs can exert a torque on the crystal grains;[16] therefore, some rotation directions of the GB must be more favorable than others. Nonetheless, a rotation of almost 90 degrees, as observed here, covered a wide spectrum of crystallographic miss-orientations between the two NPs without observing a significant difference in the migration of the GB. More importantly, quantitative measurements can be done in these experiments.

When sintering of two NPs of equal size occurs, and surface diffusion is the dominant sintering mechanism, as in this case, the surface diffusion can be expressed as:[22,23]

$$D_s = \frac{x^7 KTN_A}{56\Omega r^3 \gamma_s \delta_s t}$$

where x is the radius of the neck, K is the Boltzmann constant, T is the temperature, N_A is Avogadro's number, Ω is the atomic volume, r is the particle radius, γ_s is the surface energy, δ_s is the thickness of the surface and t is the time.

Based on the experiment in Fig. 1, we can estimate the surface diffusion coefficient by using the following data: $x = 12$ nm, $K = 1.38065 \times 10^{-23}$ J K^{-1}, $\Omega = 10.21$ cm^3 mol^{-1}, $r = 20$ nm, $\gamma_s = 1.5381$ J m^{-2},[24] $\delta_s = 1$ nm (usually 2 or 3 times the lattice spacing), and $t = 17$ s (the time elapsed in the video from Fig. 1b to d is about 11 s, but in real time it is about 17 s). For the

temperature we used $T = 308$ and estimated an error of ± 10 K to compensate for the possible change in temperature due to the electron beam. This results in a value of $7.67 \pm 0.25 \times 10^{-15}$ cm^2 s^{-1}, which is closed to previously reported values. Reported values vary from 10^{-20} cm^2 s^{-1} to 10^{-14} cm^2 s^{-1} at room temperature.[25–29] The work of Surrey *et al.*[25] is particularly interesting since the diffusion coefficient was calculated by aberration-corrected TEM observations of Au NPs below 10 nm; their result was a diffusion coefficient between 10^{-17} and 10^{-16} cm^2 s^{-1}, which is close to our results. It is important to notice that a small change in temperature will not cause a dramatic change in the surface diffusion coefficient.

We have presented a direct observation of the liquid-like behavior of a single GB at the nanoscale at room temperature, which is lower than previous reports.[15,17] After the formation of the GB fluctuations are observed with and without moving the NPs. Rotations up to 90 degrees were observed without breaking the contact between the two NPs. The free surfaces allowed the reorganization of the atoms close to the GB as one of the NPs was moved with respect to the other. Formation of a third grain was observed during the rotation of one particle due to the unfavorable crystal orientation between the two NPs. Finally, the experiments were finished when the adhesion of one of the NPs with the substrate was overcome by the stress in the NPs. Moreover, the GB was proven to be stronger than the bulk, which confirms a strong bonding between the two NPs. We used this methodology to estimate the surface diffusion coefficient in Au NPs, but it can be extrapolated to any system: two different metals, alloys, ceramics, metal–ceramics, *etc.* The mechanical manipulation of the NPs enables the study of GBs of individual NPs of any composition, and ultimately, we should be able to freely manipulate the position, composition and crystallographic orientation between nanostructures. Moreover, this approach may help experimental observation of the most basic mechanisms of GB motion in the coupling mode, GB sliding and when there is a switch between them.

Acknowledgements

The authors would like to acknowledge to the NSF-PREM Grant # DMR 0934218: "Oxide and Metal Nanoparticles – The Interface Between Life Sciences and Physical Sciences" and the Grant # DMR-1103730: "Alloys at the Nanoscale: The Case of Nanoparticles Second Phase". The authors would also like to thank the Welch Foundation grant award # AX-1615 and the NIH – RCMI: RCMI grant 5G12RR013646-12.

References

1 H. Zheng, A. Cao, C. R. Weinberger, J. Y. Huang, K. Du, J. Wang, Y. Ma, Y. Xia and S. X. Mao, *Nat. Commun.*, 2010, **1**, 144.
2 L. Lu, Y. Shen, X. Chen, L. Qian and K. Lu, *Science*, 2004, **304**, 422.
3 M. Beck, Z. Pan and B. Wetton, *Phys. D*, 2010, **239**, 1730.
4 J. Kanel, A. Novick-Cohen and A. Vilenkin, *Acta Mater.*, 2005, **53**, 227.
5 P. Liu, S. C. Mao, L. H. Wang, X. D. Han and Z. Zhang, *Scr. Mater.*, 2011, **64**, 343.
6 K. E. Harris, V. V. Singh and A. H. King, *Acta Mater.*, 1998, **46**, 2623.
7 P. M. Derlet and H. V. Swygenhoven, *Philos. Mag. A*, 2002, **82**, 1–15.
8 K. S. Kumar, S. Suresh, M. F. Chisholm, J. A. Horton and P. Wang, *Acta Mater.*, 2003, **51**, 387.
9 Z. Shan, E. A. Stach, J. M. K. Wiezorek, J. A. Knapp, D. M. Follstaedt and S. X. Mao, *Science*, 2004, **305**, 654.
10 D. S. Gianola, S. Van Petegem, M. Legros, S. Brandstetter, H. Van Swygenhoven and K. J. Hemker, *Acta Mater.*, 2006, **54**, 2253.
11 F. Mompiou, M. Legros and D. Caillard, *J. Mater. Sci.*, 2011, **46**, 4308.
12 S. Takaaki, I. Tadashi, N. Shinsuke and F. Hiroyuki, *J. Phys.: Conf. Ser.*, 2010, **258**, 012005.
13 T. Ishida, K. Kakushima and H. Fujita, *J. Appl. Phys.*, 2011, **110**, 104310.
14 Y. Lu, J. Y. Huang, C. Wang, S. Sun and J. Lou, *Nat. Nanotechnol.*, 2010, **5**, 218.
15 A. P. Merkle and L. D. Marks, *Wear*, 2008, **265**, 1864.
16 F. Wakai, H. Fukutome, N. Kobayashi, T. Misaki, Y. Shinoda, T. Akatsu, M. Sone and Y. Higo, *Acta Mater.*, 2012, **60**, 507.
17 D. W. Pashley, M. J. Stowell, M. H. Jacobs and T. J. Law, *Philos. Mag.*, 1964, **10**, 127.
18 J. W. Cahn and J. E. Taylor, *Acta Mater.*, 2004, **52**, 4887–4898.
19 E. M. Savitskii, *Handbook of Precious Metals*, Hemisphere Publishing Company, New York, 1969.
20 P. Rez and R. W. Glaisher, *Ultramicroscopy*, 1991, **35**, 65–69.
21 M. José-Yacamán, C. Gutierrez-Wing, M. Miki, D. Q. Yang, K. N. Piyakis and E. Sacher, *J. Phys. Chem. B*, 2005, **109**, 9703–9711.
22 M. A. Asoro, D. Kovar, Y. Shao-Horn, L. F. Allard and P. J. Ferreira, *Nanotechnology*, 2010, **21**, 025701.
23 M. N. Rahaman, *Ceramic Processing and Sintering*, Marcel Dekker, New York, 2003.
24 W. R. Tyson and W. A. Miller, *Surf. Sci.*, 1977, **62**, 267.
25 A. Surrey, D. Pohl, L. Schultz and B. Rellinghaus, *Nano Lett.*, 2012, **12**, 6071.
26 J. Schneir, R. Sonnenfeld, O. Marti, P. K. Hansma, J. E. Demuth and R. J. Hamers, *J. Appl. Phys.*, 1988, **63**, 717.
27 D. A. Sommerfeld, R. T. Cambron and T. P. Beebe, *J. Phys. Chem.*, 1990, **94**, 8926.
28 H. P. Hagan, P. A. Campbell, K. W. Smith, R. J. Turner and D. G. Walmsley, *Ultramicroscopy*, 1992, **42–44, Part 1**, 587.
29 H. Göbel and P. von Blanckenhagen, *Surf. Sci.*, 1995, **331–333, Part B**, 885.

Electronic Supplementary Information for

Direct observation of liquid-like behavior of a single Au grain boundary.

Gilberto Casillas, Arturo Ponce, J. Jesús Velázquez-Salazar and Miguel Jose-Yacaman

Department of Physics and Astronomy, University of Texas at San Antonio,

One UTSA Circle, San Antonio, Texas 78249, USA.

Experimental methods

We used an AFM-TEM holder from Nanofactory Instruments AB to perform the *in situ* experiments. The NPs were synthesized by a seed-mediated growth method.[1] The seeds were prepared by an aqueous mixture solution composed of 0.125 mL of 0.01 M HAuCl4 and 3.75 mL of 0.1 M CTAB, then immediately added 0.3 mL of 0.01 M NaBH4 solution, followed by rapid inversion mixing for 2 min. The resulting seed solution was kept at room temperature for 2 h before use. The seed solution was diluted 50 times with DI water. For final growth the solution was prepared by the sequential addition of 6.4 mL of 0.1 M CTAB, 0.8 mL of 0.01M HAuCl4 and 3.8 mL of 0.1 M ascorbic acid into water (32 mL). 200 μL of seed solution diluted was added to the growth solution immediately.

The NPs were drop-casted onto the tip of a 0.25 mm gold wire of 1 cm in length, which was then mounted on to a brass cap, to finally mount it in the AFM-TEM holder, as shown in Fig. S3. Once inside the TEM, the gold wire was manipulated through the Nanofactory software. The experiments were performed in a JEOL JEM-2010F equipped with a field emission gun and a Fast-Scan ATM CCD. Videos were recorded with an exposure time of 0.1 s per frame, and are displayed at a 15 frames/second rate.

The experiments consisted in applying a load to a NP with the Si tip, until it adhered to the tip. Once a good adhesion was obtained, a different NP was approached to the Si tip and brought to contact with the fixed NP. After cold-welding the NPs, the behavior of the GB was recorded in the CCD for analysis.

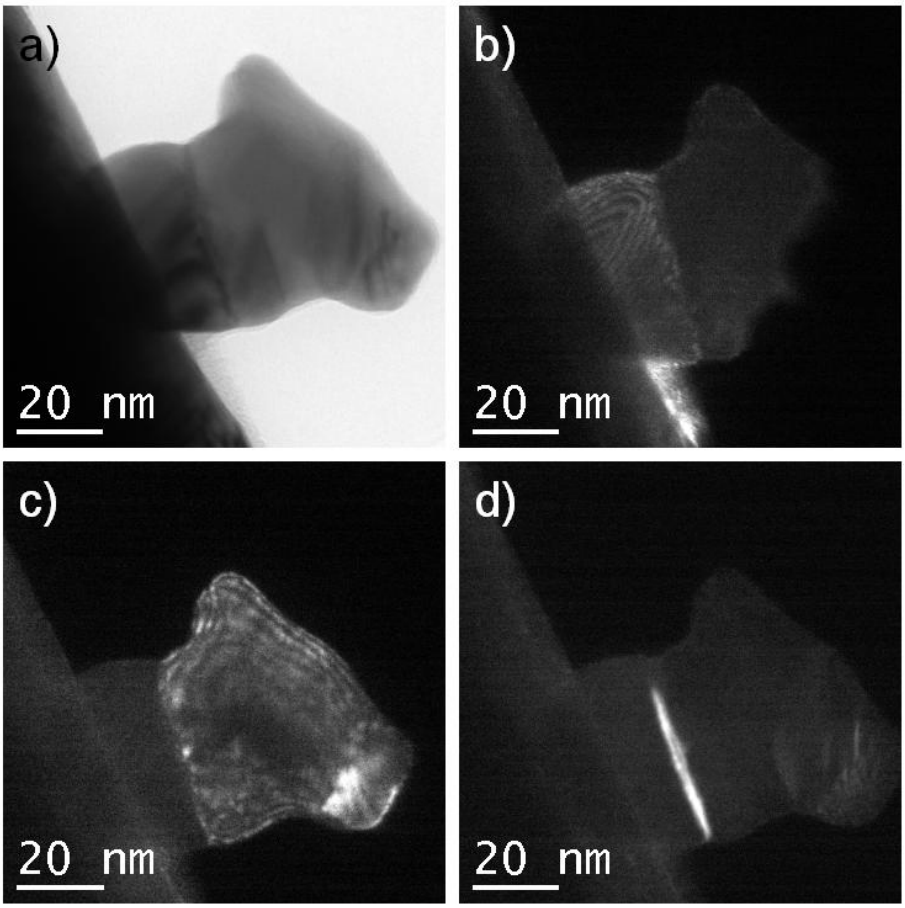

Fig. S1. (a) BF TEM image of the NPs in Fig. 1-3 after the top one detached from the silicon tip. (b) DF image of the left particle. (c) DF image of the right particle. (d) DF image of the GB.

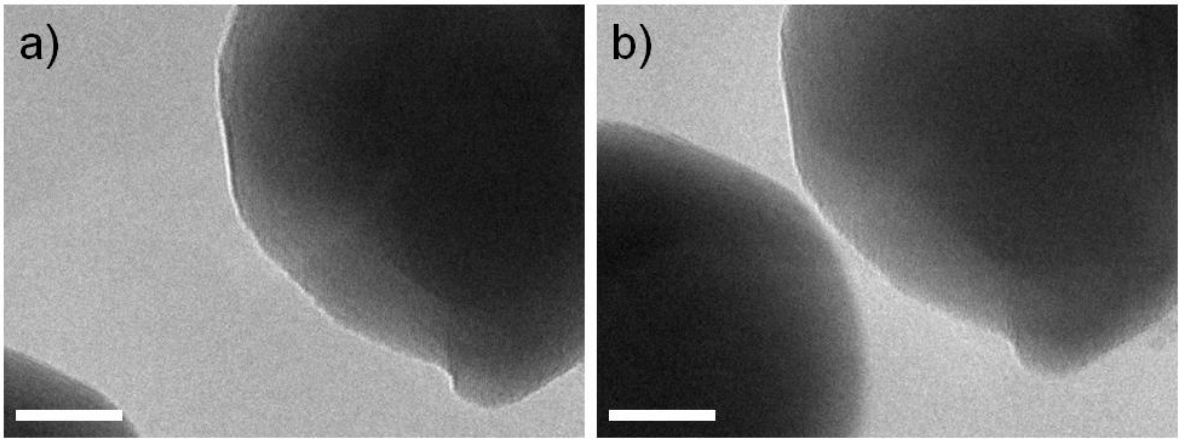

Fig.S2. TEM images of the NPs in Fig. 4 before contact. (a) Shows a frame at a time of 1 s of supplementary video 4, while (b) shows a frame at 41 s. The morphology of the NP on the right stays the same during the whole process confirming that the electron beam had no effects on the behavior of the GB. Scale bar is 10 nm.

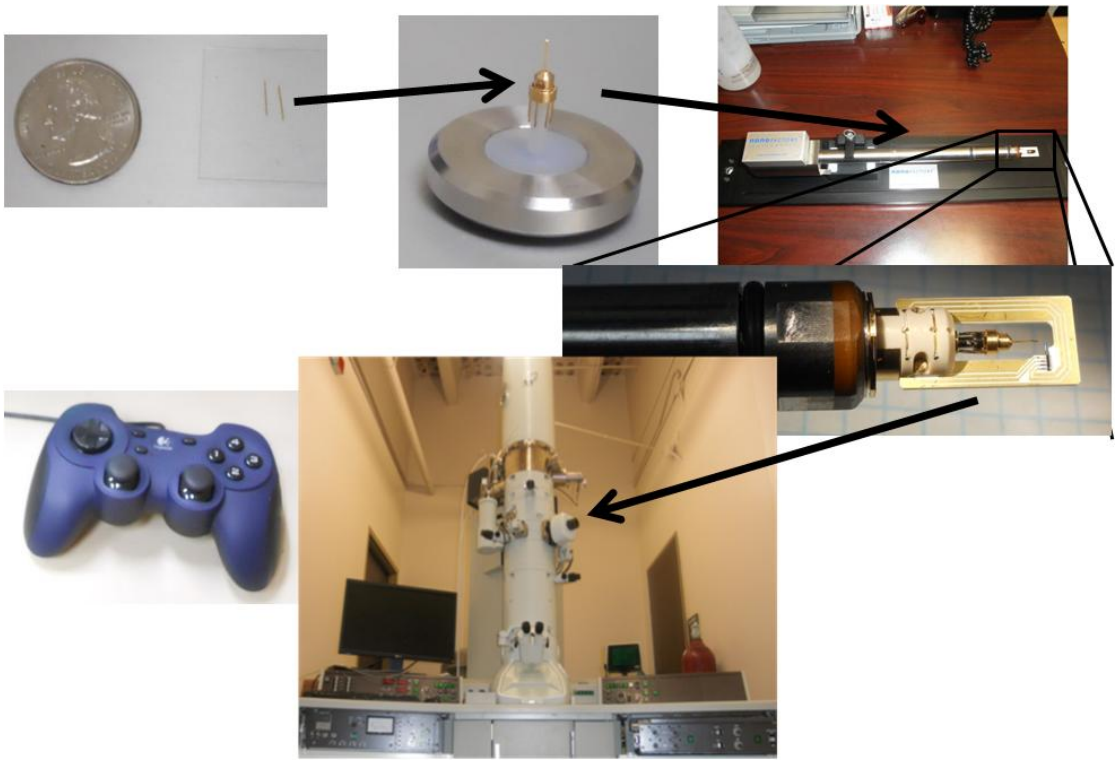

Fig. S3. Schematic of the experimental set-up.

Supplementary Video 1. TEM video of the sequences shown in Fig. 1, 2 and 3.

Supplementary Video 2. TEM video of the sequence shown in Fig. 4.

Supplementary Video 3. TEM video of the loading process of two welded NPs.

Supplementary Video 4. TEM video of the NPs in Fig. 4 before contact.

References

1 T. K. Sau, C. J. Murphy, *J. Am. Chem. Soc.*, 2004, ***126,*** 8648.

grain boundary.